Tellus (2004), 56A, 278–286
Printed in UK. All rights reserved

TELLUS

On the mid-latitude tropopause height and the orographic-baroclinic adjustment theory

By ISABELLA BORDI[1], ALESSANDRO DELL'AQUILA[1], ANTONIO SPERANZA[2] and ALFONSO SUTERA[1]*, [1]*Department of Physics, University of Rome 'La Sapienza', Piazzale Aldo Moro 2, 00185, Rome, Italy;* [2]*Department of Mathematics and Computer Science, University of Camerino, Camerino, Italy*

(Manuscript received 7 May 2003; in final form 3 February 2004)

ABSTRACT

In the extratropics the analysis of the time–space structure of the dynamical tropopause shows a marked signature of non-propagating, low-frequency (time-scale >10 d), ultra-long (zonal wavenumber <5) waves. This suggests the extension of theories relating the tropopause height to the baroclinic adjustment to the orographic-baroclinic disturbances, generally operating in the low-frequency domain. Such an extension is here proposed.

By analysing Eady modes in a Boussinesq atmosphere, it has been found that the form-drag instability must be accounted for in an extended theory of baroclinic neutralization. The produced unstable standing waves carry a poleward large amount of heat at planetary scale for most of the external parameter settings and their spatial structure strongly resembles the observed winter mid-latitude eddy fields.

Furthermore, we show how a simple representation of the stratosphere affects the tropopause neutralization requirements.

1. Introduction

In a baroclinic instability problem, when the background potential vorticity (hereafter PV) has zero meridional gradient, the geometric scale of the unstable wave is easily related to the tropopause height. Therefore, assuming that the atmosphere, on average, is close to a baroclinic neutral state, the effect of the eddies can be parametrized in terms of the tropopause height.

In a previous paper, following Lindzen (1993), Bordi et al. (2002, hereafter BDSS) exploited this property when topography is acting at the lower boundary. They showed that the inclusion of the topography and the stratosphere allows a tropopause neutrality condition behaviour more consistent with the outcomes of GCM experiments. In BDSS, however, the interaction between the zonal mean flow and the topography was not allowed. Thus, that study was restricted to the effect of topography on the 'ordinary' baroclinic instability (similar to that described, for example, in Pedlosky, 1980).

Observations of the Earth's atmosphere suggest that the process leading to this baroclinic instability is consistent with the behaviour of travelling, synoptic-scale, high-frequency disturbances (zonal wavenumber ≥ 5, time-scale <10 d). On the other hand, studies on the structure and evolution of the dynamical tropopause from observations (see, for example, Nielsen-Gammon 2001) clearly show that the ultra-long (zonal wavenumber <5) planetary waves play a relevant role on tropopause behaviour. These features are usually associated with the atmospheric low-frequency variability (time-scale ≥ 10 d) and they appear to be meridionally confined in the poleward flank of the jet core. Furthermore, on some occasions, during the Northern Hemisphere winter, these planetary-scale disturbances are known to be growing at a faster pace than the associated background flow. It has also been diagnosed that their energy source is the zonal available potential energy (Hansen, 1986) and that they strongly contribute to the total poleward heat flux (Peixoto and Oort, 1992). Furthermore, their time evolution seems to be so slowly propagating that their description as unstable standing waves may be considered more than a working assumption.

These planetary scale features (which in monthly mean maps are easily recognized as vertically coherent, but westerly tilted in the lower layers, fields) may strongly affect the mid-latitude tropopause structure. Hence, in a frame of a baroclinic adjustment theory, their effects should be, at least, considered.

In other words, it is interesting to extend the analysis shown in BDSS to a form of baroclinic conversion that might act on the scale of the low-frequency ultra-long wave disturbances. A possible candidate is the instability related to the form-drag process (Charney and Straus, 1980; Buzzi et al. 1984, and references therein). It arises when the domain integrated zonal momentum interacts at the lower boundary with the topography by producing a standing wave. The induced wave pressure-drag, in turn,

*Corresponding author.
e-mail: sutera@romatm9.phys.uniroma1.it

feeds back on to the integrated zonal momentum. This mutual re-enforcement may lead to an unstable growth (see also Section 3 for more details) during which the topography merely catalyses the required energy conversion. Because the disturbance owes its existence to the topography, the zonal scale of the growing disturbance must be similar to that of the topography. In the Northern Hemisphere, this scale is just about the one described by the first few gravest zonal Fourier modes. By its own definition, a form-drag instability may occur in the absence of a baroclinic energy source. In fact, the energy required by a growing disturbance could be drawn also from the kinetic energy of the background flow. In this case, however, the growing wave disturbance will be vertically evanescent and its growth rate is, generally, smaller than that related to the conversion of the zonal available potential energy (see Buzzi et al. 1984, and Section 2). Because observations show that, at a planetary scale, these features are troposphere filling, the study of their neutralization condition in a baroclinic environment is an appealing framework.

In terms of modelling, the study requires that, in the stability analysis, besides the potential vorticity conservation law and the associated boundary conditions, the form-drag equation must be considered. The latter is derived in a non-geostrophic frame, as it is a consequence of the momentum conservation in the presence of a surface roughness and it is related to the ageostrophic motion. In a quasi-geostrophic frame, i.e. topographic height $O(Ro)$ where Ro is the Rossby number, this equation remains applicable provided that the meridional scale of the wave disturbance is much shorter than the one characterizing the zonal momentum (Hart, 1979) and/or the meridional scales are of an infinite length. Within this framework, it will be shown that the tropopause neutralization condition discussed in BDSS is remarkably modified. The form-drag affects profoundly the baroclinic instability process leading to a neutrality condition that can be tested with more realistic models.

By restricting the analysis, as in BDSS, to a zero background tropospheric PV meridional gradient, we shall study a 'rigid lid' model (a standard Eady model with an upper lid confining the troposphere) and a 'two-layer' model (two Eady layers separated by a discontinuity in the vertical derivative of the basic fields). In these cases, the neutrality conditions can be deduced by an analytical method. When the upper layer has a constant, but nonzero, PV meridional gradient, the stability condition has been derived by a simple numerical procedure.

The paper is organized as follows. In Section 2 we present the Eady rigid lid model when the form-drag effect is taken into account. In Section 3 we show the dispersion relationship and its implications on the tropopause neutrality condition. In Section 4 we consider the consequences of the inclusion of a stratosphere. Finally, in Section 5 some sensitivity studies are performed. In a concluding section the main results are summarized and some speculative thoughts on the problem are presented.

2. Rigid lid model

To set up the frame for the study, let us review some previous works devoted to the form-drag instability problem.

Let us analyse, for example, the effects of the form-drag induced by a bottom topography h on the baroclinic instability in an Eady flow with an upper rigid lid as in Buzzi et al. (1984). Considering a Boussinesq quasi-geostrophic atmosphere in a middle latitude channel and the usual quasi-geostrophic scaling, the dimensionless PV conservation equation is

$$\frac{\mathrm{D}q}{\mathrm{D}t} = 0, \tag{1}$$

where $q = \nabla^2\psi + \partial_z(\varepsilon\partial_z\psi)$, with ψ being the quasi-geostrophic streamfunction and $\varepsilon = (L^2 f^2{}_0)/(D^2 N^2)$. Here, L and D are the horizontal and vertical scales of the flow respectively, f_0 is the Coriolis parameter at a given latitude ϕ_0 and N is the Brunt–Väisälä frequency. The domain integrated zonal momentum is assumed to be a uniform field. Therefore, its tendency is not described by eq. (1) (as, in this case, it has no vorticity). As a consequence, in order to close the problem, the form-drag equation must be considered

$$\frac{\partial \overline{u}^{x,y,z}}{\partial t} = \overline{\left(\frac{\partial\psi}{\partial x}\right)_{z=0} h}^{x,y}, \tag{2}$$

where the overbar denotes an average on the superscript variables and u is the zonal wind. In a periodic channel, the Phillips boundary conditions (Phillips, 1954; see also Pedlosky, 1979, p. 377) would imply that the right-hand side of eq. (2) is zero, unless an infinitely wide channel is considered (Hart, 1979). In physical terms, this amounts to considering the meridional scale of u to be much greater than that of ψ.[1]

The boundary conditions, at the upper lid (here identified with the tropopause height z_{T}) and at the lower boundary $z = 0$, are respectively

$$\left(\frac{\partial}{\partial t} + \boldsymbol{V}\cdot\nabla\right)\frac{\partial\psi}{\partial z} = 0, \quad \text{at} \quad z = z_{\mathrm{T}} \tag{3}$$

$$\left(\frac{\partial}{\partial t} + \boldsymbol{V}\cdot\nabla\right)\frac{\partial\psi}{\partial z} + \varepsilon^{-1}\boldsymbol{V}\cdot\boldsymbol{\nabla}h = 0 \quad \text{at} \quad z = 0, \tag{4}$$

where $\boldsymbol{V} = (u, v)$ is the horizontal component of the wind vector.

The topography (which in BDSS was operating only through the meridional slope effect as in Pedlosky, 1980) is chosen as a cosine zonal profile

$$h(x, y) = \eta G(y)(\mathrm{e}^{\mathrm{i}k_0 x} + \mathrm{e}^{-\mathrm{i}k_0 x}),$$

where $G(y)$, η and k_0 are the normalized meridional profile, the mean quasi-geostrophically scaled amplitude of the topography and its zonal wavenumber, respectively.

[1] Notice also that, if any form of dissipation is added in eq. (2), an external, globally integrated momentum source must be supplied to the system.

The basic state may include, besides the standard Eady zonal flow, an orographic wave:

$$\Psi(x, y, z) = -(u_0 + \Lambda z)y + \left[\Psi_b(z)g(y)e^{ik_0x} + \Psi_b(z)^* g(y)e^{-ik_0x}\right]. \tag{5}$$

Let $g(y)$ be the normalized meridional structure of the wave. Here, u_0 is the zonal wind at the surface and Λ is its vertical shear. Ψ_b is the stationary wave forced by topography of wavenumber k_0 and $(*)$ denotes the complex-conjugate. Its analytical expression is readily calculated (see Buzzi et al. 1984) as

$$\Psi_b(z) = \frac{\delta_{form} u_0}{\varepsilon \Delta}\{[\alpha(u_0 + \Lambda z_T) - \Lambda \tanh(\alpha z_T)]\cosh(\alpha z) + [\Lambda - \alpha(u_0 + \Lambda z_T)\tanh(\alpha z_T)]\sinh(\alpha z)\},$$

where

$$\alpha = \frac{\left(k_0^2 - \int_0^{L_y} g_{yy} g \mathrm{d}y\right)^{1/2}}{\varepsilon^{1/2}},$$

$$\delta_{form} = \eta \int_0^{L_y} g(y)G(y)\mathrm{d}y,$$

$$\Delta = \alpha z_T \Lambda^2 + \left[-\Lambda^2 + \alpha^2 u_0(u_0 + \Lambda z_T)\right]\tanh(\alpha z_T),$$

$$k_0 = \frac{2\pi s}{L_x}, \qquad L_x = 2\pi r_a \cos(\phi_0), \qquad L_y = r_a \Delta\phi.$$

Here, r_a is the dimensionless Earth's radius, $\Delta\,\phi$ is the meridional width of the jet and s is the dimensionless zonal wavenumber.

If $u_0 = 0$ the basic state is symmetric (we have no forced wave as topography operates only at $z = 0$ where the flow is zero).

Let consider the perturbation superimposed on the basic flow in the form

$$\varphi(x, y, z, t) = \left[-u'y + \Phi(z)^+ g(y)e^{ik_0x} + \Phi(z)^- g(y)e^{-ik_0x}\right] \times e^{-ik_0ct} + \text{c.c.}, \tag{6}$$

where $\Phi\,(z)^{\pm} = a^{\pm}\cosh(\alpha\,z) + b^{\pm}\sinh(\alpha z)$, $a^{\pm}$ and $b^{\pm}$ are arbitrary complex constants, and u' is the zonal component of the perturbation projecting on to the total momentum of the basic flow. Following the assumptions above, u' obeys the form-drag equation (eq. (2)). Note that the wavy part of the perturbation has both an in-phase and an out-of-phase (with respect to the topography) amplitude. Therefore, the form-drag process always produces a perturbation on the domain averaged zonal momentum.

By inserting eq. (6) in the linearized boundary conditions and in the form-drag equation, we have

$$(u_0 + \Lambda z - c)\frac{\mathrm{d}\Phi^+}{\mathrm{d}z} + u'\frac{\mathrm{d}\Psi_b}{\mathrm{d}z} - \Lambda\Phi^+ = 0 \qquad z = z_T$$

$$(u_0 + \Lambda z + c)\frac{\mathrm{d}\Phi^-}{\mathrm{d}z} + u'\frac{\mathrm{d}\Psi_b^*}{\mathrm{d}z} - \Lambda\Phi^- = 0 \qquad z = z_T$$

$$(u_0 - c)\frac{\mathrm{d}\Phi^+}{\mathrm{d}z} + u'\left(\frac{\mathrm{d}\Psi_b}{\mathrm{d}z} + \varepsilon^{-1}\delta_{form}\right) + (\delta_{slope} - \Lambda)\Phi^+ = 0 \qquad z = 0 \tag{7}$$

$$(u_0 + c)\frac{\mathrm{d}\Phi^-}{\mathrm{d}z} + u'\left(\frac{\mathrm{d}\Psi_b^*}{\mathrm{d}z} + \varepsilon^{-1}\delta_{form}\right) + (\delta_{slope} - \Lambda)\Phi^- = 0 \qquad z = 0$$

$$cu' + \delta_{form}(\Phi^+ - \Phi^-)_{z=0} = 0,$$

where a projection of the equations on to $g(y)$ has been performed. Here

$$\delta_{slope} = \frac{1}{\varepsilon}\eta \int_0^{L_y} g^2(y)\partial_y G(y)\mathrm{d}y.$$

In so far as the integrals contained in the definitions of δ_{form} and δ_{slope} are not zero, the topography acts as a potential vorticity gradient at the ground and as a tourque for the zonal momentum. The assumption that the projection of $G(y)$ over the meridional structure $g(y)$ has to be different from zero, is a necessary condition for this occurrence (see Benzi et al. 1986). Notice that BDSS is readily obtained by setting $\delta_{form} = 0$.

The system (7) is a set of five homogeneous equations for $a^{\pm}$, $b^{\pm}$ and u'. The solvability condition is

$$a_1c^5 + a_2c^3 + a_3c = 0 \tag{8}$$

where a_1, a_2 and a_3 are cumbersome functions of the parameters (not presented). When the root $c = 0$ (corresponding to the stationary solutions) is factorized out, we are left with a biquadratic equation in c. Two of its possible imaginary roots correspond to standing growing (decaying) solutions, while the others describe travelling growing (decaying) perturbations. The existence of the two purely imaginary roots is possible when the phase speed of the wave equals the wind speed at the steering level. Of course, this does not imply that there is a resonant growth, as we are studying an instability process and, therefore, the wave amplitude remains still undetermined.

Let us remark again that a 'standing' form-drag instability can occur also in the case when the wave is vertically evanescent, i.e. the Rossby height (α^{-1}) is such that the two edge waves do not 'see' each other. Of course, this type of instability will have a barotropic nature. However, more importantly, it will occur for a tropopause height lower than that obtained when a baroclinic environment is considered. Thereby, the baroclinic neutralization condition will include also the barotropic case.

The free dimensionless parameter values used hereafter are $\Lambda = 1$, $N = 1.05$, $\phi_0 = 45^\circ$ and $\Delta\,\phi = 27^\circ$.

3. Dispersion relationship and its implications on the neutrality condition

The analysis of the dispersion relationship and the spatial structure of the eigenmodes allows us to derive some useful properties

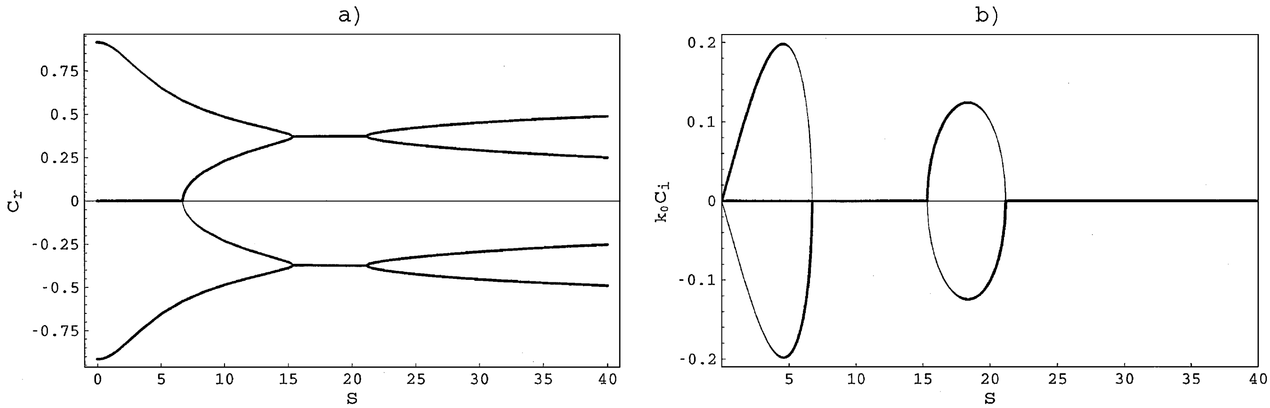

Fig 1. (a) Dimensionless real part c_r of the phase speed c and (b) growth rate $k_0 c_i$ as a function of the non-dimensional zonal wavenumber s for the 'rigid lid' model with $u_0 = 0$, $\delta_{\text{slope}} = \delta_{\text{form}} = 0.4$ and $z_T = 0.6$. The other free parameters are $\Lambda = 1$, $N = 1.05$, $\phi_0 = 45°$ and $\Delta\ \phi = 27°$.

of form-drag instability process. In Figs. 1a and b the dimensionless real part of the phase speed c, c_r, and the growth-rate, $k_0 c_i$, are plotted as functions of the non-dimensional zonal wavenumber s for a symmetric basic state ($u_0 = 0$). As already noticed, besides travelling baroclinic instability waves, a lobe of standing ($c_r = 0$) instability located in the range of ultra-long waves is present. The growth rate of the perturbation associated with the standing orographic-baroclinic instability is comparable to the travelling one. However, in the former case, the wave-scale is typical of the ultra-long waves, a feature that, in the Northern Hemisphere, is often associated with an orographic effect.

Moreover, the orographic-baroclinic instability, regardless of the u_0 value, is always operating. Inspecting the roots of the solvability condition, a few additional remarks can be made. When a non-symmetric basic state is considered, the standing instability covers a broader (narrower) region if $u_0 < 0$ ($u_0 > 0$) and the growth rate $k_0 c_i$ increases (decreases). As a consequence, a surface easterly mean zonal wind causes the standing instability to increase. The lobe of travelling unstable waves shows a greater sensitivity to the wavy part of the basic state than the standing one.[2]

Figure 2a presents the *x–z* cross-section of the standing orographic-baroclinic eigenmode. The vertical structure of the standing pattern is similar to a deep baroclinic disturbance. The vertical tilt, denoting a baroclinic conversion process, is strongly manifested in the lower troposphere, whereas a rather vertically coherent structure is present in the upper layer. Figure 2b shows the vertical structure of the long-term average (1968–1996) eddy geopotential height for January at 45°N – National Center for Environmental Prediction/National Center for Atmospheric Research (NCEP/NCAR) reanalysis data – as a function of the

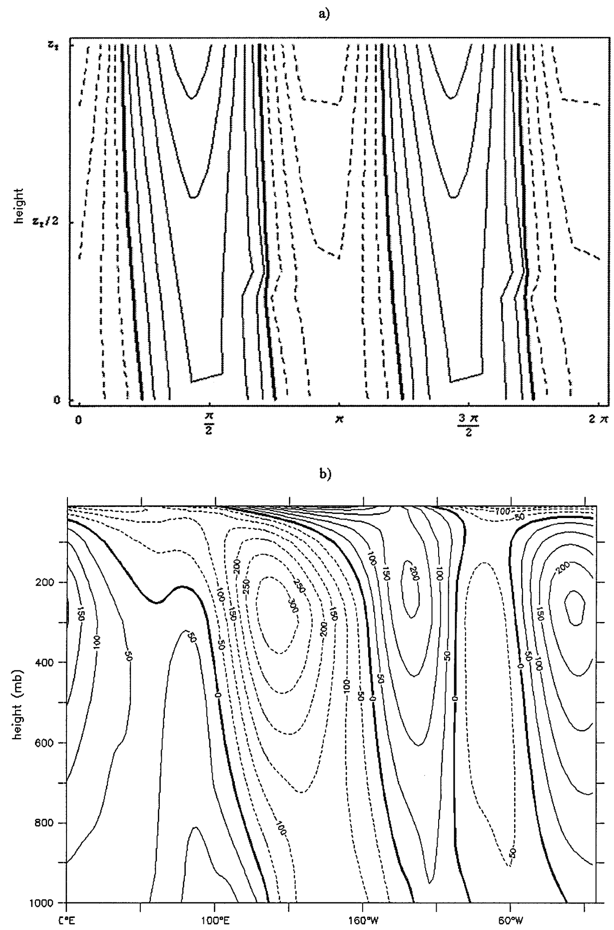

Fig 2. (a) The *x–z* cross-section of standing 'orographic-baroclinic' dimensionless eigenmode (zonal wavenumber 2). (b) The *x–p* cross-section of long-term average (1968–1996) eddy geopotential height (metres) for January at 45°N (NCEP/NCAR reanalysis data). The dashed (solid) lines pertain to negative (positive) values.

[2]This matter has consequences for baroclinic development in the presence of a wavy basic state (Bordi, 2000). The study of these important effects, however, will lead to a major digression from the aim of the present paper. Therefore, we do not deal with these any further, leaving their study to another occasion.

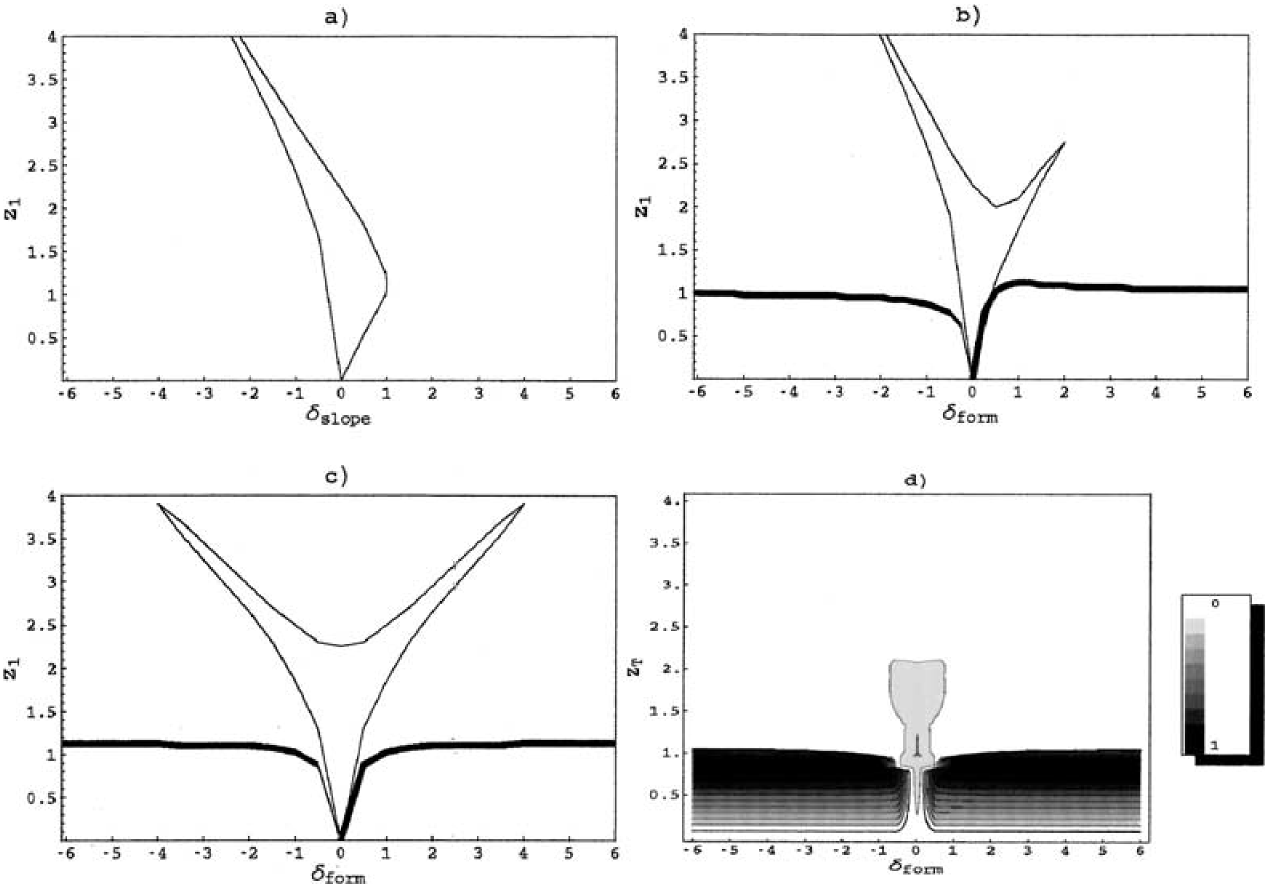

Fig 3. (a) Dimensionless z_1 as a function of δ_{slope} for $\delta_{\mathrm{form}} = 0$. (b) Dimensionless z_1 as a function of δ_{form} for $\delta_{\mathrm{form}} = \delta_{\mathrm{slope}}$. Thick lines pertain to the standing lobe. (c) Dimensionless z_1 as a function of δ_{form} where we fix $\delta_{\mathrm{slope}} = 0$. Thick lines pertain to the standing lobe. (d) Dimensionless meridional heat flux associated to the normalized baroclinic eigenmodes as a function of z_{T}. We fix $s = 1$ and $\delta_{\mathrm{slope}} = 0$. The central lobe corresponds to the travelling mode. The other free parameters are as in Fig. 1.

longitude. The two figures show encouraging similarity; in both cases, the eddy geopotential amplitude increases with height, while its phase is tilted westward mostly in the lower layer.

It is easy to show that the meridional heat flux

$$\overline{\frac{\partial \varphi}{\partial x} \frac{\partial \varphi}{\partial z}}$$

of the orographic-baroclinic eigenmode is independent of height, as it is for the classical unstable Eady waves (Pedlosky, 1979). In addition, it can be proved that, for any given s, the heat flux associated with the standing orographic disturbance is, in general, greater than that pertinent to the orographic travelling wave. All the above physical properties make the standing orographic-baroclinic process a candidate for playing a central role in the ultra-long wave dynamics. Consequently, the global structure of the dynamic tropopause might be affected by the presence of the above instability. Therefore, the tropopause neutrality condition should be considered in this wider framework. For example, a main result of BDSS was to show the importance of the effect introduced by the meridional slope of topography in the neutralization condition. It is interesting to compare the latter with the form-drag effect, as follows.

According to Section 2 of BDSS, let $z_s (s = 1, 2, \ldots)$ be the height of the tropopause for which the atmosphere is baroclinically neutral with respect to a perturbation with zonal wavenumber s. In Fig. 3a z_1 is shown as a function of δ_{slope} when no form-drag is operating ($\delta_{\mathrm{form}} = 0$). Within the area enclosed by the solid curve, there are unstable travelling perturbations. Notice that these disturbances cease to be unstable when $\delta_{\mathrm{slope}} > 1$.

In contrast, Fig. 3b shows z_1 as a function of δ_{form} (taking for instance $\delta_{\mathrm{form}} = \delta_{\mathrm{slope}}$). The thin line encloses the area of the travelling form-drag instability, while in the area underneath the bold line a standing form-drag unstable wave occurs. Hence, the range of δ_{form} for which an unstable standing disturbance exists has no upper limit. Therefore, in a complete theory, the neutrality condition must apply also to the standing disturbances. In our parameter setting, a dimensional value of $z_1 O$ (10 km) is required to achieve neutrality, a height similar to that observed in the Northern Hemisphere mid-latitude winter.

Figure 3c shows z_1 as a function of δ_{form} when $\delta_{\mathrm{slope}} = 0$. In this case only the form-drag effect is operating. Because the behaviour of z_1 is very similar to that described in Fig. 3b, for the purpose of isolating the form-drag contribution, δ_{slope} may be very well set to zero from now on.

It remains to determine whether the neutrality condition has to be applied to travelling or standing orographic instability. Figure 3d shows the dimensionless meridional heat fluxes for the standing and travelling baroclinic normalized eigenmodes (for $s = 1$) as a function of δ_{form} and z_{T}. The heat transport associated with the standing instability is about one order of magnitude greater than that pertaining to the travelling disturbance. We may conclude that the goal of a neutral tropopause is fully achieved by neutralizing the standing form-drag instability.

In leaving this section we notice that the form-drag instability disappears both for $\delta_{\mathrm{form}} = 0$ and in the limit $\delta_{\mathrm{form}} \to 0$. It may seem that the present theory would be applicable only to the Northern Hemisphere, where topography is a prominent feature. However, it can be proved (see Buzzi et al. 1984, eq. 46) that, as long as the ratio $\Lambda/\delta_{\mathrm{form}}$ remains finite, the standing form-drag instability may occur even for a small topography. Thus, we suggest that it is possible to extend the theory also to atmospheric conditions similar to those of the Southern Hemisphere, where only a small topography is present at the planetary spatial scale, but, in mid-latitude, the vertical shear of the zonal wind is, usually, large.

4. Effect of introducing a stratosphere

Following BDSS (specifically section 2.2), in this section we remove the rigid lid assumption and consider the effects of a simple representation of the stratosphere on the standing orographic-baroclinic instability process.

As described in BDSS, the equations of motion are

$$\frac{\mathrm{D}q_j}{\mathrm{D}t} = 0 \qquad \text{for} \quad j = 1, 2 \tag{9}$$

where the subscripts 1 and 2 refer to the troposphere and the stratosphere, respectively. The PV meridional gradient of the basic state is set to zero ($\partial_y \Pi_j = 0$) everywhere, except at the tropopause (where, in correspondence with the discontinuity in the zonal wind vertical shear and in the static stability, a Dirac-delta vorticity is present) and, as usual, at the ground. The boundary conditions and the form-drag equation become

$$\begin{cases} \left(\dfrac{\partial}{\partial t} + \boldsymbol{V}\cdot\nabla\right)\dfrac{\partial \psi_1}{\partial z} + \varepsilon_1^{-1}\boldsymbol{V}\cdot\boldsymbol{\nabla}h = 0 & \text{at} \quad z = 0 \\ \psi_1 = \psi_2 & \text{at} \quad z = z_{\mathrm{T}} \\ w_1 = w_2 & \text{at} \quad z = z_{\mathrm{T}} \\ \psi_2 \to 0 & \text{for} \quad z \to \infty \\ \dfrac{\partial \overline{u}^{x,y,z}}{\partial t} = \overline{\left(\dfrac{\partial \psi_1}{\partial x}\right)_{z=0} h}^{x,y} \end{cases} \tag{10}$$

with

$$\varepsilon_j = \frac{L^2 f_0^2}{D^2 N_j^2} \qquad j = 1, 2.$$

The basic state is assumed to be

$$\Psi_1 = -(u_0 + \Lambda_1 z)y + \left[\Psi_{\mathrm{b1}}(z)\mathrm{e}^{\mathrm{i}k_0 x} + \Psi_{\mathrm{b1}}(z)^*\mathrm{e}^{-\mathrm{i}k_0 x}\right] g(y) \qquad \text{for } z < z_{\mathrm{T}}$$

$$\Psi_2 = -\left[u_0 + \Lambda_1 z_{\mathrm{T}} + a_0\Lambda_1(z - z_{\mathrm{T}})\right] y + \left[\Psi_{\mathrm{b2}}(z)\mathrm{e}^{\mathrm{i}k_0 x} + \Psi_{\mathrm{b2}}(z)^*\mathrm{e}^{-\mathrm{i}k_0 x}\right] g(y) \quad \text{for } z \geq z_{\mathrm{T}},$$

where Ψ_{b1} and Ψ_{b2} are the stationary solutions of eq. (10) and a_0 is a parameter that accounts for the strength and the direction of the stratospheric zonal wind vertical shear.

Linear perturbations are then written in the form

$$\varphi_j(x, y, z, t) = \left[-u'y + \Phi_j(z)^+ g(y)\mathrm{e}^{\mathrm{i}k_0 x} + \Phi_j(z)^- g(y)\mathrm{e}^{-\mathrm{i}k_0 x}\right]\mathrm{e}^{-\mathrm{i}k_0 ct} + \text{c.c.} \tag{11}$$

with

$$\Phi_1(z)^{\pm} = a^{\pm}\cosh(\alpha_1 z) + b^{\pm}\sinh(\alpha_1 z)$$

and

$$\Phi_2(z)^{\pm} = d^{\pm}\mathrm{e}^{-\alpha_2(z - z_{\mathrm{T}})}.$$

We set

$$\alpha_j = \frac{\left(k_0^2 - \int_0^{L_y} g_{yy} g \,\mathrm{d}y\right)^{1/2}}{\varepsilon_j^{1/2}} \qquad \text{and} \qquad \gamma = \frac{N_1}{N_2}.$$

The solvability condition is

$$g_1 c^5 + g_2 c^3 + g_3 c = 0 \tag{12}$$

where g_1, g_2 and g_3 are again cumbersome functions of the parameters.

Inspecting the roots of eq. (12) it can be seen that the orographic-baroclinic instability, characterized by a non-propagating phase, is present also in this case. In fact, contours of the normalized (with respect to the solution of the rigid lid case) $z_1(\gamma, \delta_{\mathrm{form}})$ and $z_1(a_0, \delta_{\mathrm{form}})$ are plotted in Figs. 4a and b respectively (the negative δ_{form} half-plane is not displayed as it is symmetric with respect to the $\delta_{\mathrm{form}} = 0$ axis). In both figures, when δ_{form} is small, a weak dependence of z_1 on the stratospheric parameters is found while the dependence increases for $\delta_{\mathrm{form}} > 1$. Similarly to BDSS (see also Rivest et al. 1992), the introduction of the stratosphere ($\gamma \neq 0$) appears to make the baroclinic conversion less efficient, i.e. z_1 is lower than that in the corresponding rigid lid case. Moreover, by considering a stratospheric zonal wind decreasing (increasing) with height, z_1 increases (decreases). These results are in agreement with those reported in BDSS, only they apply to the standing unstable waves.

Amongst the several assumptions so far adopted, probably the least realistic one consists of the requirement that the basic state PV meridional gradient in the stratosphere is zero. In removing this limitation, let us extend the model to a constant stratospheric

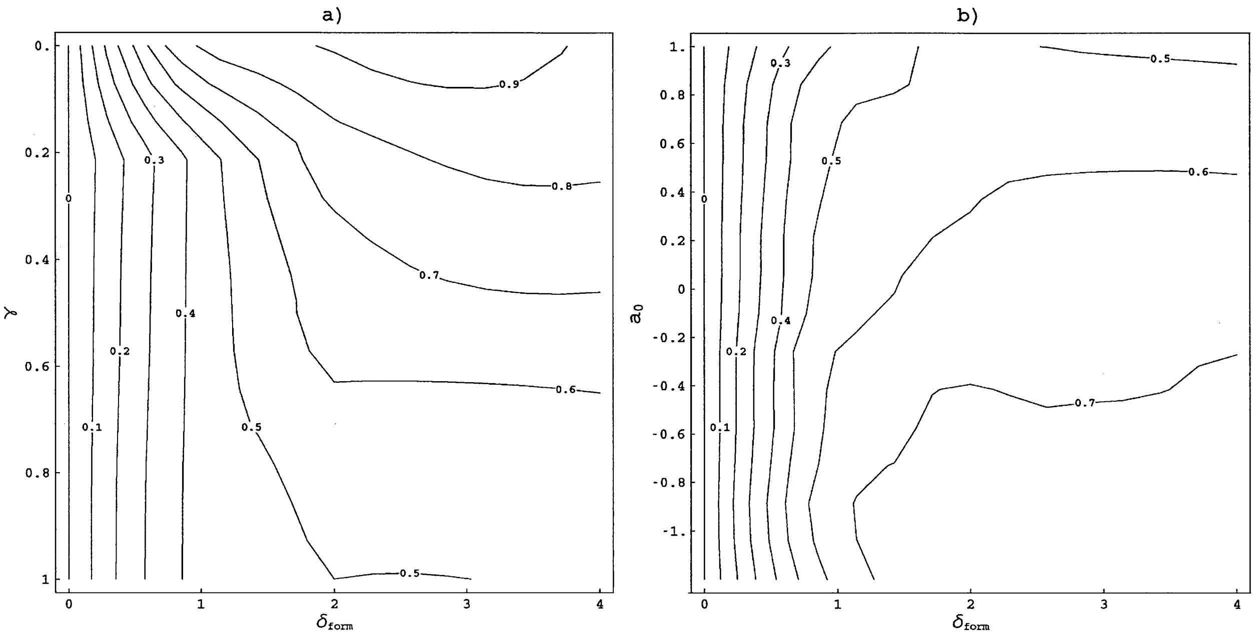

Fig 4. (a) z_1 for the 'two-layer' model normalized with respect to the corresponding 'rigid lid' case (see Fig. 3c) as a function of the static stability ratio γ and δ_{form}. We set $a_0 = 0$. (b) z_1 for the 'two-layer' model normalized with respect to the corresponding 'rigid lid' case as a function of a_0 and δ_{form}. We set $\gamma = 0.5$ and the other free parameters as in Fig. 1.

PV meridional gradient $O(\beta)$ where β is the planetary vorticity meridional gradient. The corresponding basic state zonal wind and temperature vertical profiles are determined with the same procedure adopted in BDSS.

The interior equation for the streamfunction perturbation $\Phi^{\pm}$ is

$$\partial_z \varepsilon \partial_z \Phi^{\pm} + \left(\frac{\partial_y \Pi}{u_0 + \Lambda z \mp c} - \varepsilon \alpha^2 \right) \Phi^{\pm} = 0, \tag{13}$$

where $\partial_y \Pi$ is the meridional gradient of the basic state vorticity. The lower boundary condition remains as in eq. (4). At the upper boundary we assume that a radiation condition holds

$$\partial_z \Phi^{\pm} + \mathrm{i} \sqrt{\frac{1}{\varepsilon} \left(\frac{\partial_y \Pi}{u_0 + \Lambda z \mp c} - \varepsilon \alpha^2 \right)} \Phi^{\pm} = 0 \quad \text{at} \quad z = H_{\mathrm{top}}, \tag{14}$$

where i is the imaginary unit. The form-drag equation remains as in eq. (2).

The top of the domain has been set at $H_{\mathrm{top}} = 5$ scale-heights (varying the value of H_{top} no relevant modifications were found).

The forced stationary wave Ψ_{b} (which occurs if $u_0 \neq 0$) is obtained by computing the solution $c = 0$ of eq. (13).

To solve the problem, eq. (13) is discretized by centred differences on $J = 100$ levels; the lower and upper boundary conditions are implemented by using the levels 1 and 2 and J and $J - 1$, respectively. A homogeneous system of linear equations is obtained. The phase speed c is determined by employing the solvability condition. In order to remain on the lobe of standing ($c_{\mathrm{r}} = 0$) instability, we sought solutions for c only on the imaginary axis.

A standing orographic-baroclinic solution is present also in this case. In particular, Fig. 5 shows z_1, normalized with respect to the corresponding rigid lid case, as a function of δ_{form} and $\partial_y \Pi_2/\beta$ when a symmetric basic state is considered. The result suggests that when the stratospheric $\partial_y \Pi_2$ increases, z_1 increases accordingly, especially for $\delta_{\mathrm{form}} > 1$. Moreover, the dependence of z_1 on δ_{form} is close to that described in Figs. 3 and 4 (i.e. the rigid lid and the two-layer model, respectively). When a non-symmetric basic state is used, a similar behaviour (here not shown) is obtained.

Overall, it appears that the presence of a meridional PV gradient in the stratosphere introduces an 'effective Rossby height'. An inspection of the eigenmode, in fact, shows that the disturbance decays away from the tropopause with an effective scale that is imposed both by $\partial_y \Pi_2$ and by the stratospheric vertical shear of the zonal wind.

5. Sensitivity studies

A viable method to ascertain a theory validity is to consider whether more complex atmospheric models confirm its predictions. In this section we outline the sensitivity of our results with respect to a set of external parameters that may be easily modified in a more realistic model. To this purpose, we consider the two-layer symmetric basic state. Here, we show the results sensitivity with respect to the following parameters:

(1) the Coriolis parameter f_0;
(2) the vertical wind shear Λ_1.

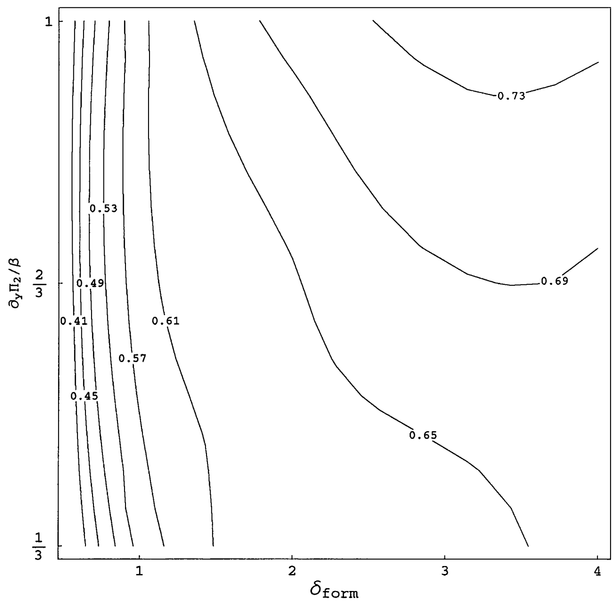

Fig 5. z_1 normalized with respect to the corresponding 'rigid lid' case as a function of δ_{form} and $\partial_y \Pi_2$ for the symmetric 'two-layer' model with a stratosphere characterized by $\partial_y \Pi_2 \neq 0$, $a_0 = 0$ and $\gamma = 0.5$.

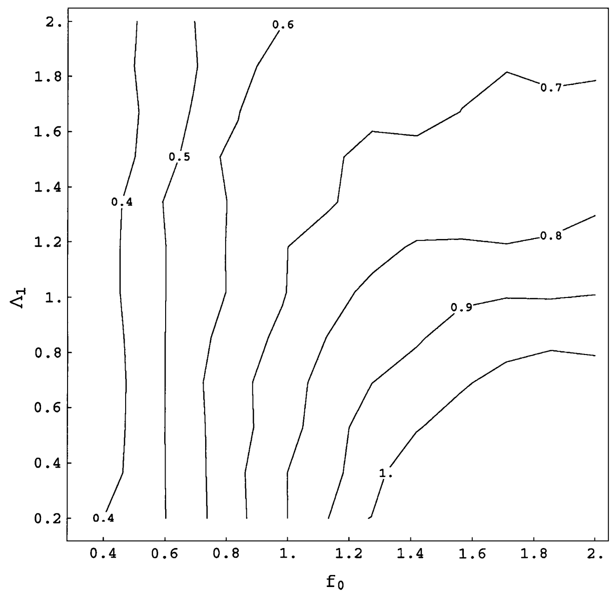

Fig 6. Dimensionless z_1 as a function of f_0 and the zonal vertical wind shear Λ_1 for the 'two-layer' model. We fix $a_0 = 0$, $\gamma = 0.5$ and $\delta_{\mathrm{form}} = 2$.

Let $a_0 = 0$, $\gamma = 0.5$, $\delta_{\mathrm{form}} = 2$ and $\partial_y \Pi_2 = 0$. Figure 6 shows z_1 as a function of f_0 and Λ_1. As in BDSS, z_1 depends on Λ_1 (i.e. on the surface meridional temperature gradient). When the planetary rotation rate is varied, z_1 increases for higher values of f_0. Thus, the neutralizing tropopause, with respect to the standing orographic-baroclinic instability, has a dependence on the Coriolis parameter, suggesting a disagreement with the GCM outcomes (Thuburn and Craig, 1997). Whether this fault may be corrected in extended theories is a questionable matter. In fact, a considerable variation of the rotation rate may drastically upset the quasi-geostrophic scaling and the associated conservation laws on which the theory is based.

We have also repeated the previous computation for the non-symmetric basic state obtaining similar results (not shown here).

6. Conclusions

In this paper a neutralization theory of the orographic-baroclinic instability has been proposed. The model appears to be structurally stable with respect to some external parameters. In fact, the orographic-baroclinic instability process always maintains its physical properties: non-propagating phase, vertical coherence, space–time scales in the range of ultra-long wave and low-frequency variability. Following the latter remark it can be speculated that the orographic instability process may account for a considerable part of the interannual variability of the observed tropopause height.

Because the form-drag effect occurs also for small topography height, we suggest that the theory can be extended to the Southern Hemisphere.

When a large topography is present, the neutrality condition on the tropopause height neutralizes also ordinary baroclinic modes of comparable wavelength. Thus, we believe that the signature of our hypothesis is more easily found in the Northern Hemisphere.

In view of the potential role of the above instability in determining the observed dynamics of the tropopause, we have devoted particular attention to its behaviour at the threshold of instability when the stratosphere is included. In this regard, we remark that the recent observed tropopause trend (Santer et al. 2003) in mid-latitudes may be connected with the present theory via the stratospheric static stability dependence of the neutralization process.

7. Acknowledgments

We acknowledge the financial support provided by the National Research Council (CNR; grant 'Accordo di Programma MURST-CNR Ecosistemi Marini') and Italian Space Agency (ASI; grants CLOUDS, GEO-MED, CASSINI and GOMAS).

Data used in Fig. 2b are NCEP/NCAR reanalysis data and have been provided by the National Oceanic and Atmospheric Administration–Cooperative Institute for Research in Environmental Sciences (NOAA–CIRES) Climate Diagnostics Center, Boulder, CO.

References

Benzi, R., Malguzzi, P., Speranza, A. and Sutera, A. 1986. The statistical properties of general atmospheric circulation: observational evidence and a minimal theory of bimodality. *Q. J. R. Meteorol. Soc.* **112**, 661–674.

Bordi, I. 2000. Regime dependent instability as a transition mechanism in large-scale atmospheric flow. *Ann. Geofis.* **43**, 135–152.

Bordi, I., Dell'Aquila, A., Speranza, A. and Sutera, A. 2002. Formula for a baroclinic adjustment theory of climate. *Tellus* **54A**, 260–272 (BDSS).

Buzzi, A., Trevisan, A. and Speranza, A. 1984. Instabilities of a baroclinic flow related to topographic forcing. *J. Atmos. Sci.* **41**, 637–650.

Charney, J. G. and Straus, D. M. 1980. Form-drag instability, multiple equilibria and propagating planetary waves in baroclinic, orographically forced, planetary systems. *J. Atmos. Sci.* **37**, 1157–1176.

Hansen, A. R. 1986. Observational characteristics of atmospheric planetary waves with bimodal amplitude distributions. *Adv. Geophys.* **29**, 101–133.

Hart, J. E. 1979. Barotropic quasi-geostrophic flow over anisotropic mountains. *J. Atmos. Sci.* **36**, 1736–1746.

Lindzen, R. S. 1993. Baroclinic neutrality and the tropopause. *J. Atmos. Sci.* **50**, 1148–1151.

Nielsen-Gammon, J. W. 2001. A visualization of the global dynamic tropopause. *Bull. Am. Meteorol.* **82**, 1151–1168.

Pedlosky, J. 1979. *Geophysical Fluid Dynamics.* Springer-Verlag, New York, 624 pp.

Pedlosky, J. 1980. The destabilization of shear flow by topography. *J. Phys. Ocean.* **10**, 1877–1880.

Peixoto, J. P. and Oort, A. H. 1992. *Physics of Climate.* Springer-Verlag, New York, 520 pp.

Phillips, N. A. 1954. Energy transformations and meridional circulations associated with simple baroclinic waves in a two-layer, quasi-geostrophic model. *Tellus* **3**, 273–286.

Rivest, C., Davis, C. A. and Farrell, B. F. 1992. Upper-tropospheric synoptic scale waves. Part I: Maintenance as Eady normal modes. *J. Atmos. Sci.* **49**, 2108–2119.

Santer, B. D., Sausen, R., Wigley, T. M. L., Boyle, J. S., AchutaRao, K. et al. 2003. Behavior of tropopause height and atmospheric temperature in models, reanalyses, and observations: Decadal changes. *J. Geophys. Res.* (D1) **108**, 1–22.

Thuburn, J. and Craig, G. C. 1997. GCM tests of theories for the height of the tropopause. *J. Atmos. Sci.* **54**, 869–882.